

2-(1*H*-1,2,3-Triazol-4-yl)-Pyridine Ligands as Alternatives to 2,2'-Bipyridines in Ruthenium(II) Complexes

Bobby Happ,^[a, b] Christian Friebe,^[a, b] Andreas Winter,^[b] Martin D. Hager,^[b]
Richard Hoogenboom,^[b] and Ulrich S. Schubert^{*[a, b]}

Abstract: The synthesis of a variety of 2-(1*H*-1,2,3-triazol-4-yl)-pyridines by click chemistry is demonstrated to provide straightforward access to mono-functionalized ligands. The ring-opening polymerization of ϵ -caprolactone initiated by such a mono-functionalized ligand highlights the synthetic potential of this class of bidentate ligands with respect to polymer chemistry or the attachment onto surfaces and nanoparticles. The coordination to Ru^{II} ions results in homoleptic and heteroleptic complexes with the resultant photophysical and electrochemical properties strongly dependent on the number of these ligands attached to the Ru^{II} core.

Keywords: click chemistry • coordination chemistry • ruthenium • UV/Vis spectroscopy • supramolecular chemistry

Introduction

The development of novel functional materials with interesting photophysical and electrochemical properties, for example, for applications in solar cells, sensors, or organic light-emitting diodes (OLEDs), represents a major challenge in current material science.^[1] Transition-metal complexes, in particular the d⁶ species such as ruthenium(II) and iridium(III) with chelating ligands, have been intensively investigated to extend the application possibilities in modern device technology. In this respect, particularly the Ru^{II} complexes of bipyridine-type ligands are highly interesting owing to their predictable photophysical and electrochemical properties.^[2] As kinetically stable bonds with bipyridines are formed, the selective synthesis of homoleptic and heteroleptic complexes is possible.^[3,4] However, the coordination of three unsymmetrical ligands can give rise to two different

conformations, that is, facial (*fac*) and meridional (*mer*) stereoisomers, which is difficult to control.^[5] In addition, the synthesis of functionalized ligands and complexes is of utmost importance. Incorporation of these ligands and complexes into polymers or the attachment onto surfaces as well as to nanoparticles can be realized through such functionalities. The covalent linking of metal complexes to a polymer backbone results in materials that combine the photophysical and electrochemical properties of the complex with the good mechanical properties of the polymer, while at the same time reducing aggregation of the complexes. Additionally, the processing features of the materials, for example, by spin coating or inkjet printing, are enhanced.^[6]

Therefore, the development of new synthetic strategies for an easy and broad access to functionalized bipyridine-type ligands is a general target of current research. The modern synthetic methodologies to obtain functionalized 2,2'-bipyridines have been reviewed recently^[1,7] and clearly reveal that the selective and easy synthesis of mono-functionalized ligands in high yields still remains a significant synthetic challenge.

Flood and co-workers have shown that the 1*H*-1,2,3-triazole moiety can be used as an alternative for pyridine in oligopyridine ligands.^[8] They have synthesized a set of 2,6-*bis*(1*H*-1,2,3-triazol-4-yl)-pyridines that utilize the Huisgen 1,3-dipolar cycloaddition,^[9] the so-called click reaction. As a comparable structure to 2,2':6',2''-terpyridines, these examples have demonstrated the versatility of this approach to substitute pyridine rings of the oligopyridine ligands by functionalized 1*H*-1,2,3-triazoles while still maintaining

[a] B. Happ, C. Friebe, Prof. Dr. U. S. Schubert
Laboratory of Organic and Macromolecular Chemistry
Friedrich-Schiller-University Jena
Humboldtstrasse 10, 07743 Jena (Germany)

[b] B. Happ, C. Friebe, Dr. A. Winter, Dr. M. D. Hager,
Dr. R. Hoogenboom, Prof. Dr. U. S. Schubert
Laboratory of Macromolecular Chemistry and Nanoscience
Eindhoven University of Technology
P. O. Box 513, 5600 MB Eindhoven (The Netherlands)
Fax: (+31) 40-2474186
E-mail: u.s.schubert@tue.nl

Supporting information for this article is available on the WWW under <http://dx.doi.org/10.1002/asia.200800297>.

metal-complexation properties.^[8] Since the early reports on the preparation of simple mono-(1*H*-1,2,3-triazole)-pyridines,^[10] various synthetic strategies based on click-type reactions as well as pharmaceutical or biomedical applications have been reported for this class of substances.^[11] Their potential usage as fluorescence sensors for transition-metal ions has very recently been introduced by Bunz and co-workers.^[12]

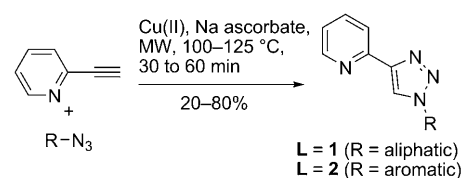
The proper combination of chelating ligands with the wide scope^[13] of the click reaction opens new avenues towards novel functional materials.^[14] To explore the applicability of this approach and to carefully investigate the properties of such functionalized (1*H*-1,2,3-triazole)-bipyridine bidentate ligands, we have synthesized a library of pyridin-2-yl substituted 1*H*-1,2,3-triazole systems **L**. Subsequently, the selective coordination of these ligands with ruthenium(II) ions has led to a full series of complexes of the general formula [Ru(dmbpy)_{3-n}(**L**)_n](PF₆)₂ (dmbpy = 4,4'-dimethyl-2,2'-bipyridine) with their photophysical and electrochemical properties strongly dependant on the number of complexed triazole-based ligands **L**. The general click protocol is also suited for the straightforward synthesis of functionalized ligands (e.g., the hydroxyl derivative **1b**) for further applications in the fields of polymer chemistry or nanotechnology.

Results and Discussion

Synthesis and Characterization

Substituted (1*H*-1,2,3-triazole)-pyridine ligands: The synthesis of the *N*^l-alkyl-substituted ligands **1** has been performed under microwave-assisted click conditions,^[15] starting from 2-ethynylpyridine and the corresponding aliphatic azide compounds, which utilize copper(II) sulfate in the presence of sodium ascorbate as the catalytic system (Scheme 1).^[9a,16] The azide compounds have been prepared from the respective alkyl bromides in a microwave-assisted nucleophilic substitution reaction by using an excess of NaN₃, and have been used without any purification or isolation. The final

Abstract in German: Die Click-Reaktion ermöglicht die Synthese von chelatisierenden, unsymmetrischen 2-(1*H*-1,2,3-Triazol-4-yl)-pyridin-Liganden, die als Strukturanaloga zu 2,2'-Bipyridinen dienen. Das große Synthesepotential dieser zweizähligen Liganden hinsichtlich möglicher Anwendungen in den Bereichen der Polymerchemie oder der Nanowissenschaft wird am Beispiel der Ringöffnungspolymerisation von ϵ -Caprolacton, initiiert durch einen derartigen, monofunktionalisierten Liganden, aufgezeigt. Homoleptische und heteroleptische Komplexe sind durch gezielte Koordinierung an Ru^{II}-Zentren zugänglich. Die photophysikalischen und elektrochemischen Eigenschaften der Komplexe weisen eine starke Abhängigkeit von der Anzahl der koordinierten neuen Liganden auf.



Scheme 1. Schematic representation of the synthesis of the bidentate (1*H*-1,2,3-triazole)-pyridine ligands **1** and **2** by click reactions (see Table 1 for details).

products **1** have been isolated in moderate to good overall yields (Table 1). For the synthesis of the aromatic derivatives **2**, a modified procedure for the one-pot click reaction

Table 1. Synthesized (1*H*-1,2,3-triazole)-pyridine ligands **1** and **2**.

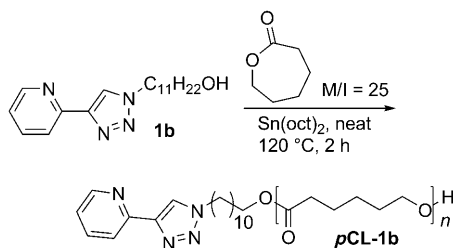
Entry	R	Yield ^[a]	Entry	R	Yield ^[a]
1a	<i>n</i> -C ₁₀ H ₂₁	79%	2a	naphthalen-1-yl	64%
1b	<i>n</i> -C ₁₁ H ₂₂ OH	66%	2b	<i>p</i> -MeO-C ₆ H ₄	44%
1c	2-(C ₂ H ₅)C ₆ H ₁₂	76%	2c	<i>p</i> -HOCH ₂ -C ₆ H ₄	20%
1d	<i>n</i> -C ₁₁ H ₂₂ COOH	21%			
1e	CH ₂ (<i>p</i> - <i>t</i> Bu-C ₆ H ₄)	66%			
1f	(CH ₂ CH ₂ O) ₄ H	22%			

[a] Yield of the isolated product after flash column chromatography (neutral Al₂O₃) and/or recrystallization (See the Supporting Information for details). TBA = tetrabutylammonium.

of boronic acids has been used.^[17] The aromatic azides have been generated in situ and subsequently reacted with 2-ethynylpyridine to give the desired *N*^l-aryl-substituted 1*H*-1,2,3-triazoles **2** in moderate yields (Scheme 1, Table 1). The purity of all of the ligands **1** and **2** has been confirmed by NMR spectroscopy, mass spectrometry, and elemental analysis. As was also concluded from the spectroscopic data, the cycloaddition has in all cases resulted in the selective formation of the 1,4-disubstituted 1*H*-1,2,3-triazoles.^[12] Notably, the mild click reaction protocol is very compatible with additional reactive functional groups (e.g., hydroxyl derivatives **1b** and **2c**). Hence, a subsequent incorporation of the synthesized ligands through these functionalities into polymers or the covalent attachment to surfaces is enabled in a straightforward manner.

Poly(ϵ -caprolactone)-containing macroligand: In recent years, various synthetic strategies to incorporate chelating ligands into polymers have been reported in the literature.^[18] In prior work, for example, we have successfully introduced polystyrene, poly(ester)s, and poly(ethylene oxide) into such materials.^[1] Among other techniques, the ring-opening polymerization (ROP) of cyclic esters, such as ϵ -caprolactone, with a hydroxy-functionalized initiator, is a suitable and efficient technique to synthesize functionalized polymers and complex polymeric architectures.^[19] With the appropriate catalyst and reaction conditions, the ROP of cyclic esters proceeds in a controlled manner. Well-defined polymers with low polydispersity indices (PDIs) and tunable molar masses are accessible by control of the reaction stoichiome-

try. Tin(II) 2-ethylhexanoate has been found to be a highly active catalyst for this kind of polymerization reaction. As a general proof of concept that the ligands can be easily introduced into polymers, we have chosen this approach to synthesize the poly(ϵ -caprolactone)-containing macroligand **pCL-1b** as summarized in Scheme 2.



Scheme 2. Schematic representation of the synthesis of the macroligand **pCL-1b** by ring-opening polymerization of ϵ -caprolactone.

The reaction has been performed in bulk monomer, using the OH-functionalized ligand **1b** as the initiator (I; M/I ratio = 25:1) and tin(II) 2-ethylhexanoate as the catalyst. Precipitation in methanol from dichloromethane has resulted in the desired macroligand **pCL-1b** in high yield (89%; the yield of the macroligand has been calculated on the basis of the initiator). The ^1H NMR spectrum of the purified polymer has confirmed the successful incorporation of the (1*H*-1,2,3-triazole)-pyridine moiety into the polymeric structure. The molar mass of the polymer ($M_n = 3,500 \text{ g mol}^{-1}$) has been calculated from the ^1H NMR spectra by comparing the integrals of the main-chain methylene groups to the resonances in the aromatic region (Figure 1). A slightly higher molar mass than the theoretical values ($M_n = 3,100 \text{ g mol}^{-1}$; predetermined from the monomer-to-initiator ratio) has been obtained. The gel-permeation chromatography (GPC)

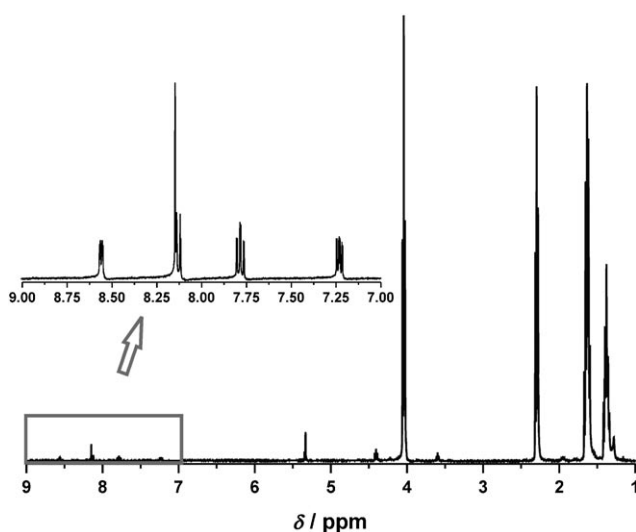


Figure 1. ^1H NMR spectrum of **pCL-1b** (400 MHz, CD_2Cl_2 , RT); the aromatic region is highlighted as an inset.

traces have been recorded with *N,N*-dimethylformamide (DMF; containing 5 mmol NH_4PF_6) as the eluent and indicated the purity of the polymeric systems with a monomodal distribution. The molar mass has been calculated by using a linear poly(ethylene oxide) calibration to be comparable with the values derived from the ^1H NMR spectrum ($M_n = 3,600 \text{ g mol}^{-1}$, PDI 1.29).

The high similarity of the GPC traces (refractive index (RI) and UV detector), together with the absorption data of **1b** and **pCL-1b**, led us to conclude that the fully ligand-functionalized material has been synthesized. However, the rather broad PDI value around 1.3 indicates that the polymerization has not proceeded in a fully controlled fashion. This observation might be explained by the limited solubility of ligand **1b** in the bulk monomer, and the increasing viscosity during the reaction resulting in hindered diffusion. The matrix-assisted laser desorption-ionization time-of-flight (MALDI-TOF) mass spectrum has additionally confirmed the incorporation of **1b** into the polymer (Figure 2). The observed molar mass distribution is in very good agreement with the theoretical value for the Na^+ ion adduct. The distance between two peaks is, in all cases, 114 Da, which fits exactly with the repeating unit of the *p*CL.

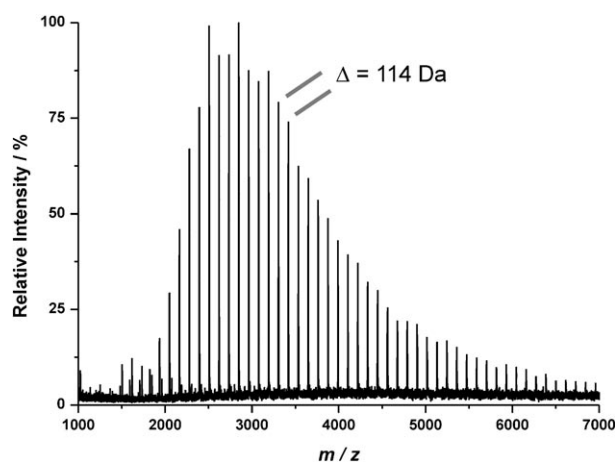
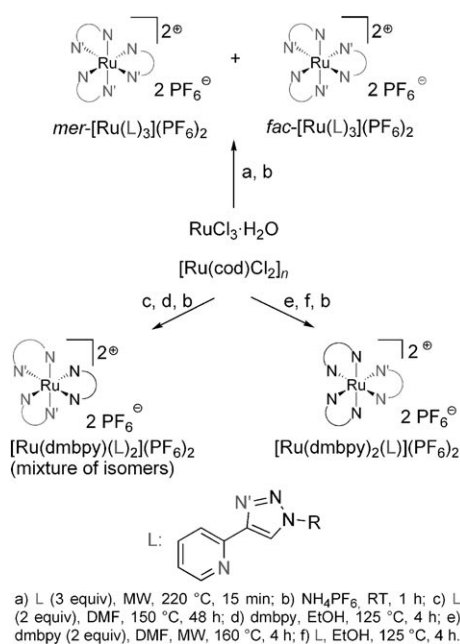


Figure 2. MALDI-TOF MS of **pCL-1b** (dithranol as the matrix).

Ruthenium(II) complexes: As already pointed out, ruthenium(II) complexes of bipyridine-type ligands are highly interesting owing to their predictable photophysical and electrochemical properties.^[2] Upon complexation, kinetically stable bonds with the ligands are formed, making the selective synthesis of homoleptic and heteroleptic complexes possible.^[3,4]

To study the influence of the (macro)ligands **L** described herein on the corresponding Ru^{II} complexes with respect to their photophysical and electrochemical properties, a series of complexes of the general formula $[\text{Ru}(\text{dmbpy})_{3-n}(\text{L})_n](\text{PF}_6)_2$ has been synthesized (Scheme 3). Therefore, we have optimized a procedure known from literature to prepare the reference complex $[\text{Ru}(\text{dmbpy})_3](\text{PF}_6)_2$ ^[20] as well as the homoleptic complexes $[\text{Ru}(\text{L})_3](\text{PF}_6)_2$ (**L** = **1** and **2**) in very



Scheme 3. Schematic representation of the syntheses of the homoleptic and heteroleptic complexes [Ru(dmbpy)_{3-n}(L)_n](PF₆)₂ (L = **1** and **2**, n = 0 to 3).

high yields by using microwave irradiation (>90%; Scheme 3). Generally speaking, the coordination of three unsymmetrical ligands will give rise to two different products, that is, facial (*fac*) and meridional (*mer*) conformers, the formation of which is difficult to control.^[5] As expected, the homoleptic *tris*-(1*H*-1,2,3-triazole)-pyridine complexes have been isolated as statistic mixtures of their two regioisomers (*fac* and *mer*). Only in the case of the bulky naphthalene-substituted ligand **2a** have we been able to separate the *fac*- and the *mer*-isomer by chromatography (SiO₂, saturated NH₄Cl in DMF/EtOH (4:1 ratio)),^[21] and the resulting NMR spectra (Figure 3) could be fully assigned by using 1D and 2D NMR techniques. Owing to the loss of symmetry, three different signals for the proton of the triazole-ring (H⁵) have been observed for the *mer*-isomer.

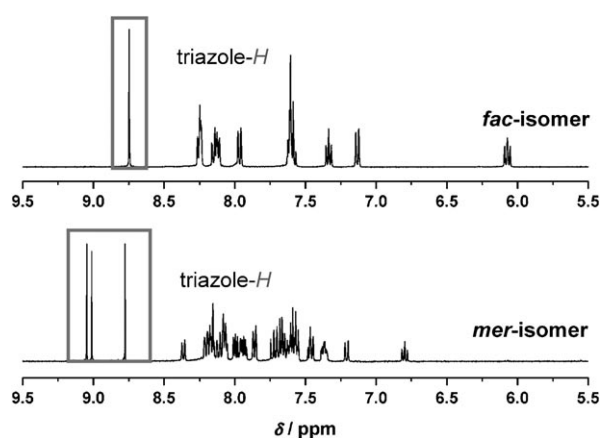


Figure 3. ¹H NMR spectra (400 MHz, CD₂Cl₂, aromatic region) of the homoleptic complexes *mer*-[Ru(**2a**)₃](PF₆)₂ and *fac*-[Ru(**2a**)₃](PF₆)₂.

As generally outlined in Scheme 3, the selective synthesis of the two different types of heteroleptic complexes involves a stepwise procedure. Therefore, [Ru(cod)Cl₂]_n (cod = 1,5-cyclooctadiene) has been converted to the precursor complexes [Ru(L)₂]Cl₂ and [Ru(dmbpy)₂]Cl₂, by reaction with the appropriate ligands in DMF under microwave irradiation. Subsequently, by microwave-assisted coordination of the respective other ligand, the heteroleptic complexes [Ru(dmbpy)₂(L)](PF₆)₂ and [Ru(dmbpy)(L)₂](PF₆)₂ have been synthesized in good yields (>80%). In this context, it is noteworthy that a complex mixture of all possible isomers, which could not previously be separated through chromatography, has been obtained for the system [Ru(dmbpy)(L)₂](PF₆)₂.

All synthesized homoleptic and heteroleptic complexes shown have been fully characterized by NMR spectroscopy, mass spectrometry, and elemental analysis. In general, all complexes have exhibited well-resolved ¹H NMR spectra with a number of characteristic features. A significant down-field shift (0.5–0.75 ppm) of the signal for the triazole-*H* (H⁵) has been observed in all cases. The same stands for the H³, H⁴, and H⁵ resonances of the pyridine rings of L, though it is less pronounced. These effects have been attributed to the induced charges, together with the π-cloud perturbation and conformational changes that occur as a consequence of the coordination of the ligand to the Ru^{II} moiety.^[8a]

Furthermore, we have successfully applied the complexation protocol for the synthesis of the heteroleptic Ru^{II} systems for the coordination of the macroligand *p*CL-**1b**. The microwave-assisted reaction has been carried out in ethanol yielding the polymer-containing complex [Ru(dmbpy)₂(*p*CL-**1b**)](PF₆)₂ in moderate yield (48%). As Ru^{II} complexes show no fragmentation on GPC columns by using optimized conditions, the macroligand complex has been investigated by this technique. A significant shift towards higher *M_n* has been obtained compared with the uncomplexed macroligand (Figure 4, top). For both compounds, mono-modal distributions have been observed. The incorporation of the Ru^{II} core into the polymer has been confirmed by applying GPC coupled with a photodiode array (PDA) detector (Figure 4, bottom). The characteristic metal-to-ligand charge-transfer (MLCT) band for such Ru^{II} complexes has been observed at around 450 nm.

The purity of the metal-containing polymer has additionally been confirmed by ¹H NMR spectroscopy. The well-resolved signals within the aromatic region (Figure 5) have been fully assigned by comparison with the related complex [Ru(dmbpy)₂(**1b**)](PF₆)₂. No impurities resulting from remaining precursor complex [Ru(dmbpy)₂]Cl₂ or uncomplexed macroligand have been detected. The molar mass as calculated from the ¹H NMR spectrum (*M_n* = 4,100 g mol⁻¹, 27 CL-repeating units) is in good agreement with the data obtained for the macroligand (28 repeating units).

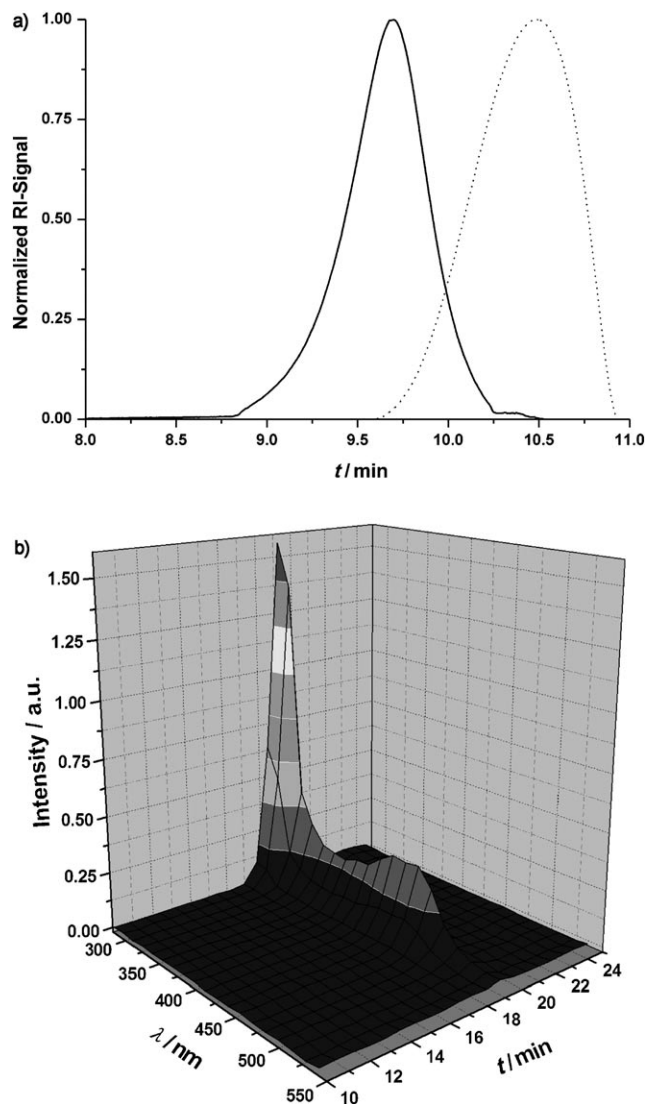


Figure 4. Top: GPC elution chromatograms of *p*CL-1b (-----) and [Ru(dmbpy)₂(*p*CL-1b)](PF₆)₂ (—). Bottom: GPC elution chromatogram of [Ru(dmbpy)₂(*p*CL-1b)](PF₆)₂ recorded with a PDA detector. For all chromatograms, 5.5 mmol NH₄PF₆ in DMF was used.

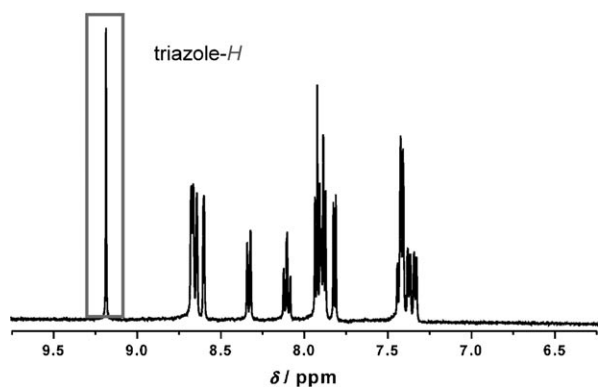


Figure 5. ¹H NMR spectrum (aromatic region) of [Ru(dmbpy)₂(*p*CL-1b)](PF₆)₂ (400 MHz, [D₆]acetone, RT).

Photophysical and Electrochemical Properties

The influence of the synthesized ligands on the photophysical and electrochemical properties of the derived Ru^{II} complexes has been investigated by UV/Vis and emission spectroscopy, as well as cyclic voltammetry. As a chromatographic separation of the configurational isomers could not, in general, be achieved, the properties are discussed for the isomeric mixtures of the respective complexes.

The UV/Vis behavior of the complexes is, in general, characterized by two strong absorption bands attributed to ligand-centered (LC, 280–300 nm) and MLCT (380–460 nm) transitions. The absorption spectra of the [Ru(dmbpy)_{3-n}(**1a**)_n](PF₆)₂ series in CH₂Cl₂ is depicted in Figure 6 (top). The homoleptic complex [Ru(**1a**)₃](PF₆)₂ shows the most pronounced blue-shift of approximately 10 nm of the LC band compared with free ligand **1a**. The same effect can be observed in the case of the MLCT bands. A distinct blue-

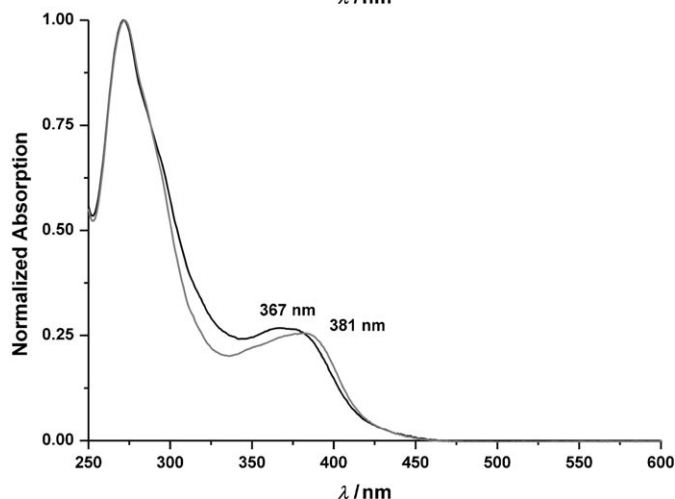
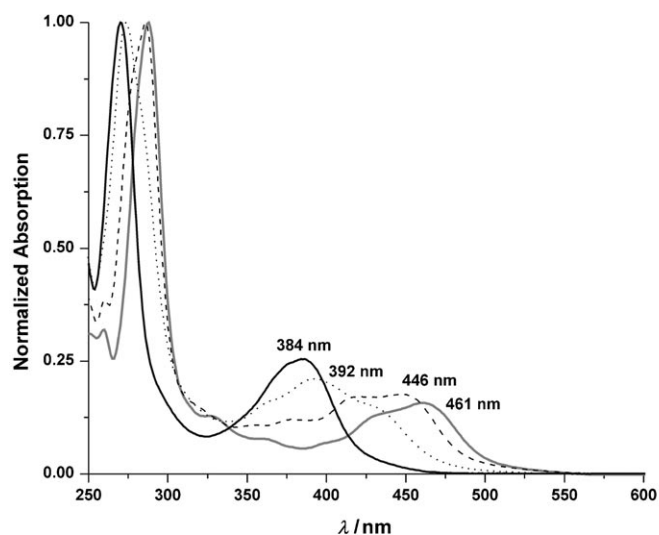


Figure 6. Top: UV/Vis absorption spectra of the [Ru(dmbpy)_{3-n}(**1a**)_n](PF₆)₂ series (*n*=3: —, *n*=2: ····, *n*=1: ----, *n*=0: —). Bottom: UV/Vis absorption spectra of [Ru(**2a**)₃](PF₆)₂ (*fac*-isomer: —, *mer*-isomer: —). For all spectra: 10⁻⁶ M of the respective complex in CH₂Cl₂ was used.

shift of this band, compared with the reference complex ($n=0$),^[22] is observed with an increasing number of (1*H*-1,2,3-triazole)-based ligands. The large relative difference of the MLCT energies for the two heteroleptic complexes can be explained by the evident transition from a dmbpy-dominated system to a more triazole-rich system (Figure 6).

As a consequence of the chromatographic separation, we have been able to determine the energetic differences of the two isomers of $[\text{Ru}(\mathbf{2a})_3](\text{PF}_6)_2$ independently (Figure 6, bottom). The MLCT band of the *mer*-isomer is blue shifted (*fac*: $\lambda_{\text{abs,max}} = 381$ nm, *mer*: $\lambda_{\text{abs,max}} = 367$ nm) and exhibits a slightly increased optical band gap (~ 0.04 eV).^[23] Obviously, the homoleptic complexes shown here are more sensitive to their coordination geometry compared with complexes based exclusively on unsymmetrical bipyridine ligands in which negligible differences between the two isomers have been reported.^[21]

Subsequently, the influence of various aliphatic and aromatic substituents on the (1*H*-1,2,3-triazole)-ring on the absorption properties of the complexes $[\text{Ru}(\text{dmbpy})_2(\mathbf{L})](\text{PF}_6)_2$ has been investigated (see the Supporting Information for details). The LC and MLCT absorption bands exhibit only small shifts upon changing the substituent on the N^1 position of the triazole moiety. Obviously, such an exchange does neither affect the $\pi_{\text{metal}}(t_{2g})$ highest occupied molecular orbital (HOMO) nor the π^* -ligands lowest unoccupied molecular orbital (LUMO). This leads to the general assumption that the π^* LUMO of these complexes is mainly located on the dmbpy ligand, and that the nature of the N^1 substituent will not have a great influence on the energy of the frontier orbitals.^[24]

The photoluminescence (PL) spectra as recorded in *n*-butyronitrile glass at 77 K have revealed strong orange emission for the heteroleptic complexes $[\text{Ru}(\text{dmbpy})_2(\mathbf{1a})](\text{PF}_6)_2$ and $[\text{Ru}(\text{dmbpy})(\mathbf{1a})_2](\text{PF}_6)_2$ with a blue-shift of 17 nm and 29 nm, respectively, compared with the homoleptic reference complex $[\text{Ru}(\text{dmbpy})_3](\text{PF}_6)_2$ ($\lambda_{\text{PL,max}} = 592$ nm, Figure 7 (top)). Owing to the experimental setup, PL quantum yields (Φ_{PL}) could not be determined. For the homoleptic complex $[\text{Ru}(\mathbf{1a})_3](\text{PF}_6)_2$, no emission has been observed.

As depicted in Figure 7 (bottom), the PL spectra shows a strong temperature dependence. A drastic decrease in the emission intensity could be observed between 150 K and 200 K, which can be attributed to the melting of the solvent matrix resulting in an increased feasibility of radiationless relaxation. In contrast with $[\text{Ru}(\text{dmbpy})_3](\text{PF}_6)_2$ ($\lambda_{\text{max,PL}} = 609$ nm, $\Phi_{\text{PL}} = 0.13$), there was no observed PL in the degassed CH_2Cl_2 solution for all of the described complexes at room temperature.

It is thought that for all dmbpy-containing heteroleptic complexes, the π^* LUMO is mainly located on the dmbpy ligand and the low-temperature PL spectra are comparable with those from bipyridine-based Ru^{II} complexes. In the case of the homoleptic complexes, $[\text{Ru}(\mathbf{L})_3](\text{PF}_6)_2$, the HOMO–LUMO transition, and thus the emission, is located on the $\pi_{\text{metal}}(t_{2g})$ HOMO and π^*_L LUMO, respectively. With an increasing number of ligands \mathbf{L} in the complex, the emis-

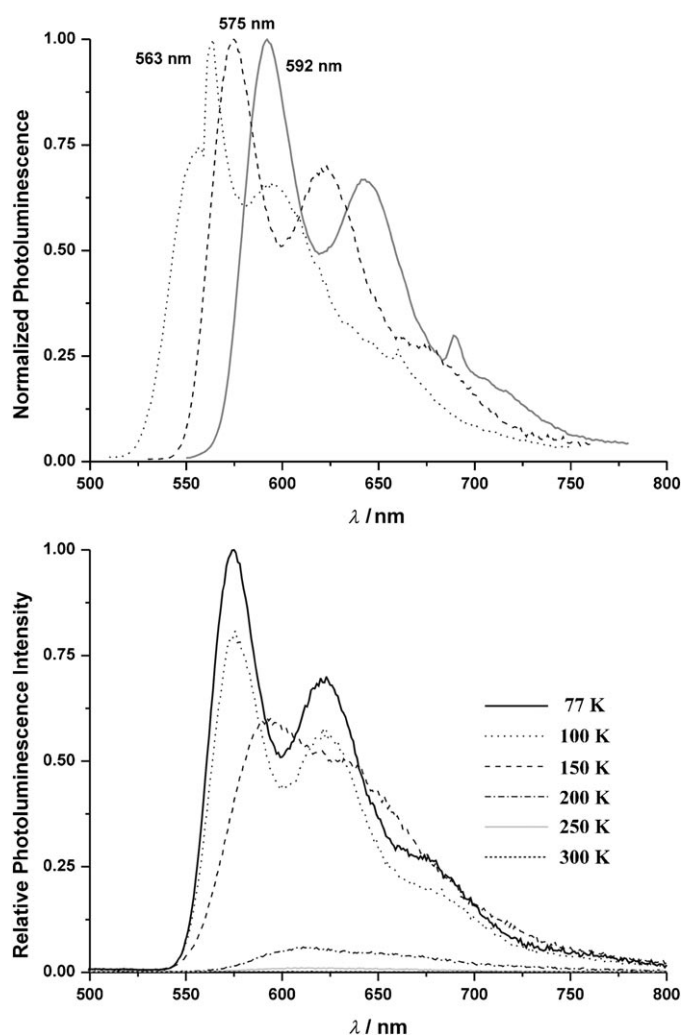


Figure 7. Top: PL spectra at 77 K of the $[\text{Ru}(\text{dmbpy})_{3-n}(\mathbf{1a})_n](\text{PF}_6)_2$ series ($n=2$: \cdots , $n=1$: $-\cdot-\cdot-$, $n=0$: $—$). Bottom: PL spectra of $[\text{Ru}(\text{dmbpy})_2(\mathbf{1a})](\text{PF}_6)_2$ at various temperatures. For all spectra, 10^{-6} M of the respective complex in *n*-butyronitrile was used.

Table 2. Electrochemical properties of the complexes $[\text{Ru}(\text{dmbpy})_{3-n}(\mathbf{L})_n](\text{PF}_6)_2$.

Entry	$E_{\text{ox}}^{\text{[a]}}$	$E_{\text{red}}^{\text{[a]}}$	HOMO ^[b]	LUMO ^[c]	E_g
$[\text{Ru}(\text{dmbpy})_3]^{2+}$	1.15 V	−1.48 V	−5.52 eV	−2.99 eV	2.53 eV
$[\text{Ru}(\text{dmbpy})_2(\mathbf{1a})]^{2+}$	1.16 V	−1.55 V	−5.55 eV	−2.93 eV	2.62 eV
$[\text{Ru}(\text{dmbpy})(\mathbf{1a})_2]^{2+}$	1.20 V	−1.64 V	−5.57 eV	−2.86 eV	2.71 eV
$[\text{Ru}(\mathbf{1a})_3]^{2+}$	1.26 V	—	−5.60 eV	—	—
<i>fac</i> - $[\text{Ru}(\mathbf{2a})_3]^{2+}$	1.44 V	—	−5.77 eV	—	—
<i>mer</i> - $[\text{Ru}(\mathbf{2a})_3]^{2+}$	1.46 V	—	−5.77 eV	—	—
$[\text{Ru}(\text{dmbpy})_2(\mathbf{1b})]^{2+}$	1.20 V	−1.50 V	−5.54 eV	−2.95 eV	2.59 eV
$[\text{Ru}(\text{dmbpy})_2(\mathbf{2a})]^{2+}$	1.24 V	−1.48 V	−5.64 eV	−2.95 eV	2.69 eV
$[\text{Ru}(\text{dmbpy})_2(\mathbf{2b})]^{2+}$	1.23 V	−1.49 V	−5.61 eV	−2.93 eV	2.69 eV

[a] Measured in degassed CH_2Cl_2 (containing 1 mM TBAPF₆) at a scan rate of 100 mV s^{−1} vs Ag/AgCl. [b] Calculated from the measured oxidation potential. [c] Calculated from the measured reduction potential.

sion energy increases and in particular, the relative PL intensity at comparable concentrations decreases.

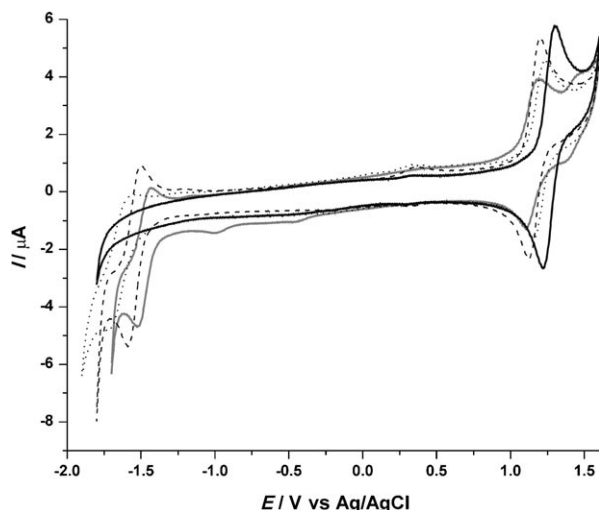


Figure 8. Cyclic voltammogram of $[\text{Ru}(\text{dmbpy})_{3-n}(\mathbf{1a})_n](\text{PF}_6)_2$ ($n=3$: —, $n=2$: ····, $n=1$: - - - -, $n=0$: — · —). For all measurements, approximately 1 mM of the respective complex in CH_2Cl_2 and 0.1 mM TBAPF₆ at 100 mV s^{-1} was employed. Yield of the isolated product after flash column chromatography (neutral Al_2O_3) and/or recrystallization (See the Supporting Information for details). TBA = tetrabutylammonium.

As seen for the photophysical properties, the electrochemical behavior of the complexes is also strongly influenced by the number of triazole-containing ligands **L** (Table 2). A single metal-based reversible oxidation step has been observed in the cyclic voltammograms (CV) for all Ru^{II} complexes (Figure 8). With an increasing number of (1*H*-1,2,3-triazole)-pyridine ligands **L**, the energy band gap E_g of the complexes increases significantly as the $\pi_{\text{metal}}(t_{2g})$ HOMO is slightly stabilized and the ligand-based π^* LUMO is significantly destabilized. As a result, no reduction peaks could be determined for the homoleptic complexes $[\text{Ru}(\mathbf{L})_3](\text{PF}_6)_2$ (**L**=**1** or **2**) within the solvent window.

The assumption that the π^* LUMO is mainly located on the dmbpy ligand is supported by the fact that no significant changes of the LUMO energies have been observed within the series of complexes of the general type $[\text{Ru}(\text{dmbpy})_2(\mathbf{L})](\text{PF}_6)_2$ (Table 2). On the other hand, the energy of the $\pi_{\text{metal}}(t_{2g})$ HOMO is significantly decreased ($\sim 0.1 \text{ eV}$) and E_g is increased to the same extent when aromatic substituents are introduced (**L**=**2a/b**).

In the case of the *fac*- and *mer*-isomer of $[\text{Ru}(\mathbf{2a})_3](\text{PF}_6)_2$, small differences for the oxidation potential (approximately 0.02 V, see the Supporting Information) but similar HOMO levels have been obtained. However, compared with the homoleptic complexes bearing *N*^l-alkyl substituents (**L**=**1a**), a remarkable decrease in the HOMO energy of 0.17 eV has been obtained. This lets us conclude that, in accordance with the $[\text{Ru}(\text{dmbpy})_2(\mathbf{L})](\text{PF}_6)_2$ series discussed above, the electrochemical properties can be influenced significantly by aryl substituents in the *N*^l position (**L**=**2**). Overall, the CV data are consistent with the previously discussed absorption/emission behavior and clearly show that the properties of

the complexes are strongly influenced by the (1*H*-1,2,3-triazole)-pyridine ligands that exhibit a significantly lower energy of the HOMO compared with analogous bipyridine-based complexes.

The photophysical and electrochemical properties of the macroligand complex $[\text{Ru}(\text{dmbpy})_2(\mathbf{pCL-1b})](\text{PF}_6)_2$ have been found to be in very good agreement with its small molecule analogue $[\text{Ru}(\text{dmbpy})_2(\mathbf{1a})](\text{PF}_6)_2$ (see the Supporting Information). Therefore, the covalent linking of the Ru^{II} complexes to the polymer backbone results in a material that now combines the photophysical and electrochemical properties of the complex with the properties of the polymer. In contrast with examples in which complexes are blended into polymer matrices, aggregation of the complexes is generally reduced. Additionally, the processing features of the materials, for example, by spin coating or inkjet printing, as well as the film-forming abilities should be strongly enhanced.

Conclusions

In conclusion, we were able to achieve the synthesis of various substituted (1*H*-1,2,3-triazole)-pyridines by a general click chemistry approach. The mild protocol is compatible with terminal functional groups that pave the way to the targeted unsymmetrical, mono-functionalized ligands, which can furthermore be easily introduced into polymers or attached to surfaces. To generally prove this concept, the incorporation of such a mono-functionalized ligand into a polymer was carried out through the ring-opening polymerization of ϵ -caprolactone. A full series of homoleptic and heteroleptic Ru^{II} complexes was derived from the bidentate ligands. In this case, the chromatographic separation of the *fac* and *mer* isomer of a homoleptic Ru^{II} complex was achieved in the case of bulky naphthalene substituents.

The question, if (1*H*-1,2,3-triazol-4-yl)-pyridines can be effectively used as alternative ligands to 2,2'-bipyridines in Ru^{II} complexes, was answered by investigating the photophysical and electrochemical properties of the synthesized complexes. A strong dependency on the number of coordinated (1*H*-1,2,3-triazole)-pyridine ligands was revealed. Overall, the synthesized ligands were found to stabilize the HOMO of the derived complexes leading to a significant increase of the energy-band gap. Together with the reversible redox properties, the complexes mainly resemble their bipyridine-based counterparts, but with distinctive differences. The complexes containing the (1*H*-1,2,3-triazole)-pyridine and bearing at least one bipyridine ligand exhibited a strong orange emission at low temperatures. In contrast with conventional Ru^{II} *tris*-bipyridine complexes, this photoluminescence is fully quenched at room temperature.

The combination of functionalized (1*H*-1,2,3-triazol-4-yl)-pyridines with ruthenium(II) ions opens new avenues for the design of new supramolecular architectures. Their applicability as functional materials, for example, photovoltaic devices, needs to be the focus of further investigation.

Experimental Section

General Methods

All reagents were purchased from commercial sources and used without further purification unless specified. The solvents were received from Biosolve and were dried and distilled according to standard procedures. The syntheses of the ruthenium(II) complexes $[\text{Ru}(\text{cod})\text{Cl}_2]_n$, $[\text{Ru}(\text{dmbpy})_2]\text{Cl}_2$ and $[\text{Ru}(\text{dmbpy})_3](\text{PF}_6)_2$ were carried out according to the literature.^[20,25] Chromatographic separations were performed on aluminum oxide (neutral, Macherey & Nagel, 0.063–0.200 mm). Preparative layer chromatography (PLC) was performed on silica gel (SiO₂ 60 on 20×20 cm² glass plates, 1-mm layer thickness, Merck).

Instrumentation

The 1D (¹H and ¹³C) and 2D NMR (gCOSY) spectra were recorded in deuterated solvents (Cambridge Isotope Laboratories Inc.) at 25 °C on a Varian Mercury 400 MHz instrument and reported in ppm relative to TMS as reference. Matrix-assisted laser desorption-ionization time-of-flight mass spectrometry (MALDI-TOF MS) was performed on a Voyager-DE PRO biospectrometry workstation (Applied Biosystems) time-of-flight mass spectrometer reflector, with dithranol as a matrix. High-resolution electrospray ionization mass spectrometry (HR-ESI MS) was carried out on a Finnigan MAT 95XL machine. Elemental analyses were obtained on a EuroVector EuroEA3000 elemental analyzer for CHNS-O. Gel permeation chromatograms were obtained using a Waters GPC equipped with an isocratic pump, a solvent degasser, a column oven, a 2996 photodiode array (PDA) detector, a 2414 refractive index detector, a 717plus autosampler, and a styragel HT4 GPC column with a pre-column installed (DMF, 5 mmol NH₄PF₆, 50 °C, flow rate of 0.5 mL min⁻¹, poly(ethylene oxide) calibration). UV/Vis spectra were measured on a Perkin-Elmer Lambda-19 spectrometer, room temperature photoluminescence spectra were recorded on a Perkin-Elmer LS50B luminescence spectrometer. Absolute quantum yields were evaluated on a Hamamatsu Photonic Multi-Channel Analyzer C10027. For these three techniques, a concentration of 10⁻⁶ M in degassed CH₂Cl₂ (1 cm cuvette) at 25 °C was used. Low-temperature emission measurements were performed on an Edinburgh Instruments FS 920 Fluorescence Spectrometer. Therefore, solutions were prepared in non-degassed *n*-butyronitrile. The experimental set-up allowed the measurement of PL spectra at arbitrary temperatures between 77 K and room temperature. Electrochemical experiments were carried out by using an Autolab PGSTAT30 potentiostat at a scan rate of 100 mV s⁻¹. For this, a standard three-electrode configuration was used with a platinum disk working electrode, a platinum-rod auxiliary electrode, and an Ag/AgCl reference electrode. Ferrocene was added at the end of each experiment as an internal standard. The potentials are quoted vs. the Fc/Fc⁺ couple. The solvent was CH₂Cl₂, containing tetra-*n*-butylammonium hexafluorophosphate (*n*Bu₄NPF₆, 0.1 M).

Safety Comment

Sodium azide is very toxic; personal protection precautions should be taken. As low-molecular-weight organic azides are potential explosives, care must be taken during their handling. Generally, when the total number of carbon (*n_C*) plus oxygen (*n_O*) atoms is less than the total numbers of nitrogen atoms (*n_N*) by a ratio of three, that is, (*n_C*+*n_O*)/*n_N* ≤ 3, the compound is considered as an explosive hazard. Therefore, the compounds were prepared prior to use and used immediately.

Synthesis

1: *N*¹-alkyl-substituted 1*H*-1,2,3-triazoles. Sodium azide (1.2 equiv), 1-bromoalkane (2 mmol); the resulting azides are **potentially explosive** in the cases of (*n_C*+*n_O*)/*n_N* ≤ 3 and 2-ethynylpyridine (1 equiv) were suspended in EtOH/water (8 mL, 7:3 ratio) in a 20 mL microwave vial. Subsequently, CuSO₄·5H₂O (23 mg, 5 mol %) and sodium ascorbate (90 mg, 25 mol %) were added. The reaction mixture was heated under microwave irradiation at 125 °C for 20 min. After cooling to room temperature, water (15 mL) was added to the brownish suspension. The precipitate was filtered off and washed with water (3×5 mL). The crude product was

further purified by gel filtration (Al₂O₃, CH₂Cl₂ as the eluent), followed by precipitation from CH₂Cl₂ into *n*-pentane. For full characterization of **1a–f** and variational experimental details, see the Supporting Information.

2: *N*¹-aryl-substituted 1*H*-1,2,3-triazoles. Sodium azide (6 mmol) and anhydrous CuSO₄ (62 mg, 0.4 mmol) were dissolved in absolute methanol (15 mL) in a 20-mL microwave vial. The aromatic boronic acid (3.84 mmol) was added to the brown solution and the mixture was stirred for 17 h at room temperature. The conversion of the reaction was monitored by TLC (SiO₂, CHCl₃ as eluent). Then CuSO₄·5H₂O (30 mg, 0.2 mmol), sodium ascorbate (384 mg, 1.95 mmol), 2-ethynylpyridine (4.2 mmol), and water (5 mL) were added. The reaction mixture was heated under microwave irradiation at 100 °C for 1 h. Water (30 mL) was added and the product was extracted with toluene (3×15 mL). After drying (MgSO₄) and evaporation of the solvent, the crude product was purified by column chromatography (Al₂O₃, CH₂Cl₂/EtOAc (1:1 ratio) as eluent). For full characterization of **2a–c** and variational experimental details, see the Supporting Information.

Macroligand pCL-1b by ring-opening polymerization of ε-caprolactone:

A degassed solution of **1b** (30 mg, 0.095 mmol) in bulk ε-caprolactone (freshly distilled, 0.251 mL, 2.37 mmol, 25 equiv) in a sealed 5-mL microwave vial was heated to 120 °C. A catalytic amount of tin(II) 2-ethylhexanoate (2 drops) was added by using a syringe and stirring was continued at 120 °C for 2 h. The crude polymer was dissolved in CH₂Cl₂ (5 mL) after cooling to room temperature. Precipitation into methanol yielded the desired polymer **pCL-1b** as a white powder (276 mg, 89%). ¹H NMR (400 MHz, CD₂Cl₂): δ = 1.25–1.41 (m, polymer backbone), 1.55–1.66 (m, polymer backbone), 2.25–2.33 (m; polymer backbone), 3.95–4.09 (m; polymer backbone), 4.41 (t, ³J_{H,H} = 7.2 Hz, 2H; H^a), 7.23 (ddd, ³J_{H,H} = 7.5 Hz, ³J_{H,H} = 4.9 Hz, ⁴J_{H,H} = 1.2 Hz, 1H; H^b), 7.78 (m_c, 1H; H^c), 8.13 (m_c, 1H; H^d), 8.15 (s, 1H; H^e), 8.56 ppm (ddd, ³J_{H,H} = 4.9 Hz, ⁴J_{H,H} = 1.8 Hz, ⁵J_{H,H} = 1.0 Hz, 1H; H^f); MS (MALDI-TOF): *M*_{max}(*m/z*) = 2,849. GPC: *M*_n = 3,600 g mol⁻¹ (PDI = 1.29).

[Ru(1a)₂]Cl₂: $[\text{Ru}(\text{cod})\text{Cl}_2]_n$ (140 mg, 0.5 mmol) and **1a** (280 mg, 0.98 mmol) were suspended in dry and degassed DMF (20 mL). The suspension was refluxed at 150 °C for 48 h. After cooling to room temperature, the precipitate was filtered off and washed with acetone (2×10 mL) and diethyl ether (2×10 mL). $[\text{Ru}(\mathbf{1a})_2]\text{Cl}_2$ was obtained as a dark-green powder (204 mg, 56%). ¹H NMR and ¹³C NMR spectra: Owing to the very low solubility in most organic solvents, no NMR spectra could be obtained. MS (MALDI-TOF): *m/z*: 674.02 [*M*–2Cl]⁺, 708.96 [*M*–Cl]⁺, 898.95 [*M*–2Cl+dithranol]⁺; elemental analysis: calcd (%) for C₃₄H₅₂Cl₂N₈Ru: C 54.83, H 7.04, N 15.04; found: C 54.93, H 7.31, N 15.02.

[Ru(1a)₃](PF₆)₂: A solution of RuCl₃·H₂O (10 mg, 0.038 mmol) and **1a** (33 mg, 0.115 mmol) in degassed ethylene glycol (6 mL) was irradiated under microwave conditions at 220 °C for 30 min. The yellow solution was treated with NH₄PF₆ (10-fold excess). The precipitate was isolated by filtration, washed with water (5 mL) and diethyl ether (10 mL) yielding the homoleptic complex $[\text{Ru}(\mathbf{1a})_3](\text{PF}_6)_2$ as a yellow solid (97%, 46 mg, mixture of the facial and meridional isomer). A chromatographic separation of the isomers could not be achieved. UV/Vis (CH₂Cl₂): λ(ε) = 385 (15,590), 270 nm (61,200). ¹H NMR (400 MHz, CD₂Cl₂): δ = 0.89 (m_c, 12H; H^a), 1.21–1.36 (m, 42H; H^b), 1.90 (m_c, 6H; H^b), 4.39 (m_c, 6H; H^a), 7.25 and 7.34 (2 m_c, 3H; H^{pyridine}), 7.71 and 7.78 (2 m_c, 3H; H^{pyridine}), 7.93 and 8.00 (2 m_c, 3H; H^{pyridine}), 8.13 (m_c, 4H; H^{pyridine}), 8.50, 8.56, 8.62 and 8.67 ppm (4 s, 3H; H^c); ¹³C NMR (CD₂Cl₂, 100 MHz): δ = 13.8, 22.6, 26.0, 26.1, 26.3, 28.8, 28.9, 29.3, 29.4, 29.5, 29.6, 29.7, 31.9, 52.4, 52.5, 52.6, 52.67, 52.9, 121.7, 122.0, 122.4, 122.7, 123.7, 124.1, 124.6, 124.9, 125.0, 125.8, 125.9, 137.6, 138.0, 138.1, 147.7, 148.1, 148.2, 151.3, 151.4, 151.5, 151.7, 151.8, 152.3 ppm; MS (MALDI-TOF MS): *m/z* = 674.20 [*M*–1a–2PF₆]⁺, 898.22 [*M*–1a–2PF₆+matrix]⁺, 1105.32 [*M*–PF₆]⁺; elemental analysis: calcd (%) for C₅₁H₇₈F₁₂N₆P₂Ru: C 48.99, H 6.29, N 13.44; found: C 49.29, H 6.44, N 13.26.

[Ru(2a)₃](PF₆)₂: A solution of RuCl₃·H₂O (20 mg, 0.076 mmol) and **2a** (62 mg, 0.230 mmol) in degassed ethylene glycol (12 mL) was irradiated under microwave conditions at 220 °C for 15 min. The yellow solution was treated with NH₄PF₆ (10-fold excess). After 1 h of stirring at room temperature, the precipitate was isolated by filtration and washed with

water (5 mL) and diethyl ether (10 mL) to yield the homoleptic complex [Ru(**2a**)₃](PF₆)₂ as a yellow solid (81 mg, 89%, mixture of the facial and meridional isomer). Chromatographic separation of the isomers was performed by PLC (SiO₂, saturated NH₄Cl in DMF/EtOH (4:1 ratio) as the eluent). The pure isomers (*fac*: $R_f = 0.2$, 45 mg, 56%; *mer*: $R_f = 0.5$, 36 mg, 44%) were isolated by extraction with a solution of NH₄PF₆ (10 mol%) in acetone for 2 h, followed by precipitation in diethyl ether.

fac-[Ru(**2a**)₃](PF₆)₂: UV/Vis (CH₂Cl₂) $\lambda(\epsilon) = 385$ (14,400), 272 (56,200); 295 nm (35,250); ¹H NMR (400 MHz, CD₂Cl₂): $\delta = 6.07$ (ddd, ³J_{H,H} = 8.3 Hz, ³J_{H,H} = 6.9 Hz, ⁴J_{H,H} = 1.2 Hz, 1H; H⁵), 7.13 (dd, ³J_{H,H} = 8.5 Hz, ⁴J_{H,H} = 0.7 Hz, 1H; H⁶), 7.34 (ddd, ³J_{H,H} = 8.1 Hz, ³J_{H,H} = 6.9 Hz, ⁴J_{H,H} = 1.0 Hz, 1H; H⁴), 7.61 (m_c, 3H; H^{naph}), 7.96 (d, ³J_{H,H} = 8.3 Hz, 1H; H³), 8.14 (m_c, 2H; H^{naph}), 8.25 (m_c, 2H; H^{naph}), 8.75 ppm (s, 1H; H⁷); ¹³C NMR (100 MHz, CD₂Cl₂): $\delta = 121.1$, 123.0, 123.9, 124.9, 126.6, 126.7, 127.2, 128.2, 128.3, 128.5, 131.9, 132.3, 134.0, 138.6, 148.4, 151.3, 152.0 ppm; MS (MALDI-TOF): $m/z = 435.86$ [M-L-2PF₆+matrix]²⁺, 645.91 [M-L-2PF₆+H]⁺, 870.88 [M-L-2PF₆+matrix]⁺, 1062.86 [M-PF₆]⁺; MS (HR-ESI) m/z calcd for C₅₁H₃₆P⁹⁶RuF₆N₁₂ [M-PF₆]: 1057.1907; found: 1057.1911.

mer-[Ru(**2a**)₃](PF₆)₂: UV/Vis (CH₂Cl₂) $\lambda(\epsilon) = 368$ (16,190), 272 (59,270), 295 nm (38,800); ¹H NMR (400 MHz, CD₂Cl₂): $\delta = 6.80$ (m_c, 1H), 7.21 (d, ³J_{H,H} = 9.5 Hz, 1H), 7.37 (m_c, 2H), 7.47 (m_c, 2H), 7.55–7.75 (m, 10H), 7.86 (d, ³J_{H,H} = 8.2 Hz, 2H), 7.92–8.02 (m, 4H), 8.05–8.21 (m, 10H), 8.36 (d, ³J_{H,H} = 8.1 Hz, 1H), 8.78 (s, 1H; H⁷), 9.01 (s, 1H; H⁷), 9.05 ppm (s, 1H; H⁷); ¹³C NMR (100 MHz, CD₂Cl₂): $\delta = 120.8$, 120.9, 122.4, 122.7, 123.6, 124.1, 124.3, 124.5, 124.9, 125.2, 125.8, 125.9, 126.4, 126.8, 127.0, 127.3, 127.4, 127.5, 127.6, 128.1, 128.2, 128.4, 128.6, 128.7, 128.8, 131.9, 132.0, 132.2, 132.3, 134.0, 134.2, 134.3, 138.1, 138.3, 138.6, 148.4, 148.8, 150.9, 151.2, 152.1, 152.4, 152.6 ppm; MS (MALDI-TOF): $m/z = 435.86$ [M-2a-2PF₆+matrix]²⁺, 645.91 [M-L-2PF₆+H]⁺, 870.88 [M-L-2PF₆+matrix]⁺, 1062.86 [M-PF₆]⁺; MS (HR-ESI) m/z calcd for C₅₁H₃₆P⁹⁶RuF₆N₁₂ [M-PF₆]: 1057.1907; found: 1057.1911.

General procedure for [Ru(dmbpy)₂(L)](PF₆)₂: A suspension of [Ru(dmbpy)₂](Cl₂) (0.08 mmol) and the triazole-pyridine ligand **L** (0.08 mmol) in degassed ethanol (8 mL) was heated at 125 °C under microwave irradiation for 1 h. The clear red solution was treated with a 10-fold excess of NH₄PF₆ and stirred for 2 h until precipitation occurred. The precipitate was filtered off and washed with ethanol (2 × 5 mL) and diethyl ether (2 × 10 mL), followed by recrystallization from acetonitrile/diethyl ether (3:1), to yield the heteroleptic complex [Ru(dmbpy)₂(L)](PF₆)₂.

[Ru(dmbpy)₂(1a**)](PF₆)₂**: Yield: 72%; UV/Vis (CH₂Cl₂) $\lambda(\epsilon) = 451$ (12,530), 413 (11,900), 286 (71,500), 260 nm (27,750); ¹H NMR (400 MHz, CD₂Cl₂): $\delta = 0.89$ (t, ³J_{H,H} = 6.9 Hz, 3H; H⁹), 1.15–1.31 (m, 14H; H^{c-h}), 1.86 (m_c, 2H; H^b), 2.56 and 2.59 (2 s, 12H; H^{methoxy}), 4.38 (t, ³J_{H,H} = 7.4 Hz, 2H, H⁷), 7.15 (dd, ³J_{H,H} = 5.8 Hz, ⁴J_{H,H} = 0.8 Hz, 1H; H^{dmbpy}), 7.23–7.31 (m, 4H; H⁴, H^{dmbpy}), 7.52 (d, ³J_{H,H} = 5.8 Hz, 1H; H^{dmbpy}), 7.56 (d, ³J_{H,H} = 5.5 Hz, 1H; H⁷), 7.56–7.62 (m, 3H; H^{dmbpy}), 7.95 (m_c, 1H; H⁵), 8.13 (m_c, 1H; H⁵), 8.14 (s, 1H; H^{dmbpy}), 8.18 (s, 1H; H^{dmbpy}), 8.23 (s, 2H; H^{dmbpy}), 8.65 ppm (s, 1H; H⁷); ¹³C NMR (100 MHz, CD₂Cl₂): $\delta = 13.8$, 21.0, 21.1, 22.6, 26.2, 28.7, 29.2, 29.3, 29.4, 29.5, 31.8, 52.5, 122.7, 124.0, 124.3, 124.6, 124.7, 125.1, 125.9, 127.6, 128.4, 128.4, 128.5, 128.7, 137.9, 147.4, 149.7, 150.3, 150.3, 150.4, 150.6, 150.8, 150.9, 151.1, 156.2, 156.3, 156.7, 156.8, 156.9 ppm; MS (HR-ESI) m/z calcd for C₄₁H₃₀P⁹⁶RuF₆N₈ [M-PF₆]: 895.2876; found: 895.2833; elemental analysis: calcd (%) for C₄₁H₃₀F₁₂N₈P₂Ru: C 47.08, H 4.78, N 10.71; found: C 47.23, H 4.78, N 10.69.

[Ru(dmbpy)₂(1b**)](PF₆)₂**: Yield: 90%; UV/Vis (CH₂Cl₂) $\lambda(\epsilon) = 418$ (10,200), 380 (7,500), 286 (70,600), 261 (32,400) 249 nm (28,720); ¹H NMR (400 MHz, CD₂Cl₂): $\delta = 1.18$ –1.30 (m, 12H; H^{c-h}), 1.52 (m, 4H; H^b, H⁹), 1.86 (m_c, 2H; H^b), 2.56, 2.58, 2.59 (3 s, 12H; H^{methoxy}), 3.59 (t, ³J_{H,H} = 6.6 Hz, 2H; H⁹), 4.38 (t, ³J_{H,H} = 7.4 Hz, 2H; H⁹), 7.15 (dd, ³J_{H,H} = 5.8 Hz, ⁴J_{H,H} = 0.8 Hz, 1H; H^{dmbpy}), 7.23–7.31 (m, 4H; H⁴, H^{dmbpy}), 7.52 (d, ³J_{H,H} = 5.8 Hz, 1H; H^{dmbpy}), 7.56–7.62 (m, 4H; H⁵, H^{dmbpy}), 7.94 (dd, ³J_{H,H} = 7.8 Hz, ⁴J_{H,H} = 1.4 Hz 1H; H⁵), 8.13 (d, ³J_{H,H} = 7.8 Hz, 1H; H⁴), 8.16 & 8.20 & 8.24 & 8.26 (4 brs, 4H; H^{dmbpy}), 8.67 ppm (s, 1H; H⁷); ¹³C NMR (100 MHz, CD₂Cl₂): $\delta = 18.2$, 20.9, 21.0, 21.1, 25.7, 26.1, 28.7, 29.2, 29.3, 29.4, 29.5, 32.8, 52.5, 62.7, 122.7, 124.0, 124.3, 124.7, 124.8, 125.1, 125.9, 127.6, 128.4, 128.5, 128.6, 137.9, 149.8, 150.3, 150.4, 150.5,

150.8, 150.9, 151.0, 151.1, 156.3, 156.7, 156.8, 156.9, 157.1 ppm; MS (MALDI-TOF): $m/z = 602.17$ [M-2PF₆-dmbpy+H]⁺, 695.04 [M-2PF₆-tripy+matrix]⁺, 786.18 [M-2PF₆]⁺, 931.12 [M-PF₆]⁺; elemental analysis: calcd (%) for C₄₂H₃₂F₁₂N₈OP₂Ru: C 46.89, H 4.87, N 10.41; found: C 47.09, H 5.17, N 10.06.

[Ru(dmbpy)₂(2a**)](PF₆)₂**: Yield: 79%; UV/Vis (CH₂Cl₂) $\lambda(\epsilon) = 430$ (10,610), 286 (60,230), 260 nm (19,420); ¹H NMR (400 MHz, CD₃CN): $\delta = 2.44$ (s, 3H; H^{methoxy}), 2.58 (s, 3H; H^{methoxy}), 2.60 (s, 3H; H^{methoxy}), 2.61 (s, 3H; H^{methoxy}), 7.12 (m_c, 2H), 7.29–7.38 (m, 4H), 7.53 (m_c, 1H), 7.58 (d, ³J_{H,H} = 5.8 Hz, 1H), 7.66–7.78 (m, 6H), 7.96 (d, ³J_{H,H} = 5.8 Hz, 1H), 8.05 (m_c, 1H), 8.09 (d, ³J_{H,H} = 8.3 Hz, 1H), 8.20 (m_c, 2H), 8.25 (s, 1H), 8.37 (s, 1H), 8.41 (s, 2H), 9.08 ppm (s, 1H, H⁷); ¹³C NMR (100 MHz, CD₃CN): $\delta = 20.1$, 20.2, 20.3, 20.4, 121.1, 122.8, 124.1, 124.3, 124.5, 124.8, 124.9, 125.0, 125.3, 126.1, 127.4, 127.5, 127.6, 127.9, 128.1, 128.2, 128.3, 128.4, 128.6, 131.7, 132.3, 134.1, 138.0, 148.1, 150.0, 150.2, 150.3, 150.4, 150.9, 151.1, 151.2, 151.6, 151.8, 156.5, 156.9, 156.9, 157.2 ppm; MS (MALDI-TOF): $m/z = 695.17$ [M-2a-2PF₆+matrix]⁺, 742.22 [M-2PF₆+Na]⁺, 887.19 [M-PF₆]⁺; elemental analysis: calcd (%) for C₄₁H₃₆F₁₂N₈P₂Ru: C 47.53, H 3.52, N 10.86; found: C 47.38, H 3.86, N 11.02.

[Ru(dmbpy)₂(2b**)](PF₆)₂**: Yield: 90%; UV/Vis (CH₂Cl₂) $\lambda(\epsilon) = 417$ (10,370), 285 (80,440), 260 nm (30,100); ¹H NMR (400 MHz, CD₃CN): $\delta = 2.54$ (s, 3H; H^{methoxy}), 2.55 (s, 3H; H^{methoxy}), 2.57 (s, 3H; H^{methoxy}), 2.58 (s, 3H; H^{methoxy}), 3.85 (s, 3H; H^{methoxy}), 7.09 (d, ³J_{H,H} = 8.5 Hz, 2H, H^b), 7.20 (dd, ³J_{H,H} = 5.8 Hz, ⁴J_{H,H} = 1.1 Hz, 1H; H^{dmbpy}), 7.29 (d, ³J_{H,H} = 5.8 Hz, 3H; H^{dmbpy}), 7.33 (m_c, 1H; H⁵), 7.61–7.67 (m, 5H; H⁵, H^a, H^{dmbpy}), 7.71 (d, ³J_{H,H} = 5.8 Hz, 1H; H^{dmbpy}), 7.83 (d, ³J_{H,H} = 5.8 Hz, 1H; H^{dmbpy}), 8.03 (dd, ³J_{H,H} = 7.8 Hz, ⁴J_{H,H} = 1.4 Hz, 1H; H⁵), 8.30 (d, ³J_{H,H} = 7.8 Hz, 1H; H⁶), 8.34 (s, 1H; H^{dmbpy}), 8.37 (s, 1H; H^{dmbpy}), 8.41 (s, 1H; H^{dmbpy}), 8.42 (s, 1H; H^{dmbpy}), 9.51 ppm (s, 1H; H⁷); ¹³C NMR (100 MHz, CD₃CN): $\delta = 20.3$, 55.5, 114.9, 122.4, 122.6, 123.9, 124.2, 124.6, 124.8, 124.9, 125.9, 127.4, 128.1, 128.3, 129.5, 137.9, 148.3, 149.9, 150.1, 150.2, 150.9, 151.0, 151.1, 151.2, 151.4, 151.6, 156.5, 156.9, 156.9, 157.2, 160.8 ppm; MS (MALDI-TOF): $m/z = 469.91$ [M-2PF₆-2b]⁺, 537.89 [M-2PF₆-dmbpy]⁺, 694.89 [M-2PF₆-2b+matrix]⁺, 721.93 [M-2PF₆]⁺, 866.83 [M-PF₆]⁺; elemental analysis: calcd (%) for C₃₈H₃₆F₁₂N₈OP₂Ru: C 45.11, H 3.59, N 11.08; found: C 44.85, H 3.84, N 10.72.

[Ru(dmbpy)₂(1a**)₂](PF₆)₂**: A suspension of [Ru(**1a**)₂](Cl₂) (30 mg, 0.04 mmol) and dmbpy (8 mg, 0.042 mmol) in degassed ethanol (6 mL) was heated under microwave irradiation at 125 °C for 4 h. The red solution was filtered through a pipette filled with a cotton pad. The clear filtrate was treated with NH₄PF₆ (10-fold excess) to give a precipitate, which was purified by column chromatography (Al₂O₃, CH₂CN as eluent). Precipitation from the concentrated acetonitrile solution in diethyl ether afforded [Ru(dmbpy)₂(**1a**)₂](PF₆)₂ (mixture of isomers, 36 mg, 78%). UV/Vis (CH₂Cl₂) $\lambda(\epsilon) = 393$ (13,700), 361 (10,000) 286 (47,300), 273 (65,400), 240 nm (34,900); ¹H NMR (400 MHz, CD₂Cl₂): $\delta = 0.89$ (t, ³J_{H,H} = 6.9 Hz, 6H; H⁹), 1.16–1.36 (m, 28H; H^{c-h}), 1.82–1.95 (m, 4H; H^b), 2.57–2.61 (m, 6H; H^{methoxy}), 4.40 (m_c, 4H; H⁹), 7.15–7.35 (m, 4H), 7.57–7.73 (m, 4H), 7.87–7.99 (m, 2H), 8.04–8.23 (m, 4H), 8.59 (s, 1H), 8.62 (s, 1H), 8.67 (s, 1H), 8.70 ppm (s, 1H); ¹³C NMR (100 MHz, CD₂Cl₂): $\delta = 13.8$, 21.1, 22.6, 26.2, 28.7, 29.2, 29.3, 29.4, 29.5, 29.6, 31.8, 52.6, 122.1, 122.3, 122.4, 122.7, 122.8, 123.6, 123.9, 124.3, 124.5, 124.7, 124.9, 125.1, 125.2, 125.8, 125.9, 127.5, 127.7, 128.4, 137.6, 138.0, 147.4, 147.7, 147.8, 149.7, 149.8, 150.3, 150.4, 150.8, 151.0, 151.1, 151.2, 151.4, 151.5, 151.6, 151.7, 156.7, 157.1, 157.2 ppm; MS (MALDI-TOF): $m/z = 572.21$ [M-2PF₆-1a+H]⁺, 797.22 [M-2PF₆-1a+matrix]⁺, 1003.32 [M-PF₆]⁺; elemental analysis: calcd (%) for C₄₆H₆₄F₁₂N₁₀P₂Ru: C 48.12, H 5.62, N 12.02; found: C 48.29, H 5.42, N 11.97.

[Ru(dmbpy)₂(pCL-1b)](PF₆)₂: A suspension of [Ru(dmbpy)₂](Cl₂) (26 mg, 0.046 mmol) and pCL-1b (80 mg, 0.02 mmol) in degassed ethanol (6 mL) was heated under microwave irradiation at 125 °C for 8 h. The reaction mixture was filtered through a pad of glass wool. An excess of NH₄PF₆ (10 equiv) was then added and after 2 h the precipitation was completed by adding water. The red precipitate was filtered off and dissolved in acetone. The solution was concentrated and precipitated in cold methanol to yield pure [Ru(dmbpy)₂(pCL-1b)](PF₆)₂ (45 mg, 48%). ¹H NMR (400 MHz, [D₆]acetone): $\delta = 1.33$ –1.42 (m; polymer backbone), 1.55–1.63 (m; polymer backbone), 2.26–2.35 (m; polymer backbone), 2.57 (m_c,

12H; H^{methy}), 4.05 (m_c; polymer backbone), 4.52 (t, ³J_{H,H} = 7.1 Hz, 2H; H^β), 7.33–7.45 (m, 5H; H^{dmppy}, H^δ), 7.82 (d, ³J_{H,H} = 5.8 Hz, 1H; H^{dmppy}), 7.87–7.94 (m, 4H; H^{dmppy}, H^β), 8.11 (dt, ³J_{H,H} = 7.9 Hz, ⁴J_{H,H} = 1.4 Hz, 1H; H^β), 8.33 (d, ³J_{H,H} = 7.9 Hz, 1H; H^δ), 8.60 (s, 1H; H^{dmppy}), 8.64 (s, 1H; H^{dmppy}), 8.67 (s, 1H; H^{dmppy}), 8.68 (s, 1H; H^{dmppy}), 9.19 ppm (s, 1H; H^δ); MS (MALDI-TOF): M_{max}(m/z) = 3014.

Acknowledgements

The authors acknowledge financial support from the Nederlandse Organisatie voor Wetenschappelijk Onderzoek (VICI award for U.S.S.) and the Fonds der Chemischen Industrie. We also thank Manuela Chiper (GPC), Rebecca Eckardt (elemental analysis), Tina Erdmenger (MALDI-TOF MS), Nicole Herzer (MALDI-TOF MS), and Christoph Ulbricht (NMR spectroscopy) for discussion and help with the respective measurements.

- [1] V. Marin, E. Holder, R. Hoogenboom, U. S. Schubert, *Chem. Soc. Rev.* **2007**, *36*, 618–635.
- [2] V. Balzani, A. Juris, M. Venturi, *Chem. Rev.* **1996**, *96*, 759–833.
- [3] P. D. Rillema, K. B. Mack, *Inorg. Chem.* **1982**, *21*, 3849–3854.
- [4] E. A. Seddon, K. Seddon, *The Chemistry of Ruthenium*, Elsevier Science Publishers B. V., Amsterdam **1984**.
- [5] N. C. Fletcher, M. Nieuwenhuyzen, S. Rainey, *J. Chem. Soc. Dalton Trans.* **2001**, 2641–2648.
- [6] a) B.-J. de Gans, P. C. Duineveld, U. S. Schubert, *Adv. Mater.* **2004**, *16*, 203–213; b) S. Y. Yang, M. F. Rubner, *J. Am. Chem. Soc.* **2002**, *124*, 2100–2101.
- [7] G. R. Newkome, A. K. Patri, E. Holder, U. S. Schubert, *Eur. J. Org. Chem.* **2004**, *2*, 235–254.
- [8] a) Y. Li, J. C. Huffman, A. H. Flood, *Chem. Commun.* **2007**, *26*, 2692–2694; b) Y. Li, A. H. Flood, *Angew. Chem. Int. Ed.* **2008**, *47*, 2649–2652.
- [9] a) J. H. Boyer, J. Hamer, *J. Am. Chem. Soc.* **1955**, *77*, 951–954; b) R. Huisgen, R. Knorr, L. Möbius, G. Szeimies, *Chem. Ber.* **1965**, *98*, 4014–4021; c) R. Huisgen, G. Szeimies, L. Möbius, *Chem. Ber.* **1967**, *100*, 2494–2507.
- [10] a) D. Seebach, D. Enders, R. Dach, R. Pieter, *Chem. Ber.* **1977**, *110*, 1879–1886; b) D. Haebich, W. Barth, M. Roesner, *Heterocycles* **1989**, *29*, 2083–2088.
- [11] a) I. Perez-Castro, O. Caamano, F. Fernandez, M. D. Garcia, C. Lopez, E. De Clercq, *Org. Biomol. Chem.* **2007**, *5*, 3805–3813; b) K. El Akri, K. Bougrin, J. Balzarini, A. Faraj, R. Benhida, *Bioorg. Med. Chem. Lett.* **2007**, *17*, 6656–6659; c) A. Goeminne, M. McNaughton, G. Bal, G. Surpateanu, P. Van der Veken, S. De Prol, W. Versees, J. Steyaert, S. Apers, A. Haemers, K. Augustyns, *Bioorg. Med. Chem. Lett.* **2007**, *17*, 2523–2526; d) A. Romero, C.-H. Liang, Y.-H. Chiu, S. Yao, J. Duffield, S. J. Sucheck, K. Marby, D. Rabuka, P. Y. Leung, Y.-K. Shue, Y. Ichikawa, C.-K. Hwang, *Tetrahedron Lett.* **2005**, *46*, 1483–1487; e) C.-H. Liang, S. Yao, Y.-H. Chiu, P. Y. Leung, N. Robert, J. Seddon, P. Sears, C.-K. Hwang, Y. Ichikawa, A. Romero, *Bioorg. Med. Chem. Lett.* **2005**, *15*, 1307–1310; f) W. J. L. Wood, A. W. Patterson, H. Tsuruoka, R. K. Jain, J. A. Ellman, *J. Am. Chem. Soc.* **2005**, *127*, 15521–15527; g) J. Li, M. Zheng, W. Tang, P.-L. He, W. Zhu, T. Li, J.-P. Zuo, H. Liu, H. Jiang, *Bioorg. Med. Chem. Lett.* **2006**, *16*, 5009–5013; h) P. van der Peet, C. T. Gannon, I. Walker, Z. Dinev, M. Angelin, S. Tam, J. E. Ralton, M. J. McConville, S. J. Williams, *ChemBioChem* **2006**, *7*, 1384–1391; i) L. Cosyn, K. K. Palaniappan, S.-K. Kim, H. T. Duong, Z.-G. Gao, K. A. Jacobson, S. Van Calenbergh, *J. Med. Chem.* **2006**, *49*, 7373–7383; j) J. Xie, C. T. Seto, *Bioorg. Med. Chem.* **2007**, *15*, 458–473; k) F. Dolhem, M. J. Johansson, T. Antonsson, N. Kann, *J. Comb. Chem.* **2007**, *9*, 477–486.
- [12] D. Schweinfurth, H. I. Hardcastle, U. H. F. Bunz, *Chem. Commun.* **2008**, *27*, 2203–2205.
- [13] a) C. J. Hawker, K. L. Wooley, *Science* **2005**, *309*, 1200–1205; b) V. Aucagne, K. D. Hanni, D. A. Leigh, P. J. Lusby, D. B. Walker, *J. Am. Chem. Soc.* **2006**, *128*, 2186–2187; c) W. R. Dichtel, O. S. Miljanic, J. M. Spruell, J. R. Heath, J. F. Stoddart, *J. Am. Chem. Soc.* **2006**, *128*, 10388–10390; d) P. Mobian, J. P. Collin, J.-P. Sauvage, *Tetrahedron Lett.* **2006**, *47*, 4907–4909; e) N. K. Devaraj, P. H. Dinolfo, C. E. D. Chidsey, J. P. Collman, *J. Am. Chem. Soc.* **2006**, *128*, 1794–1795; f) P. Wu, V. V. Fokin, *Aldrichim. Acta* **2007**, *40*, 7–17; g) U. Monkowius, S. Ritter, B. König, M. Zabel, H. Yersin, *Eur. J. Inorg. Chem.* **2007**, *29*, 4597–4606; h) O. David, S. Maisonnette, J. Xie, *Tetrahedron Lett.* **2007**, *48*, 6527–6530.
- [14] D. Fournier, R. Hoogenboom, U. S. Schubert, *Chem. Soc. Rev.* **2007**, *36*, 1369–1380.
- [15] a) V. V. Rostovtsev, L. G. Green, V. V. Fokin, K. B. Sharpless, *Angew. Chem.* **2002**, *114*, 2708–2711; *Angew. Chem. Int. Ed.* **2002**, *41*, 2596–2599; b) T. R. Chan, R. Hilgraf, K. B. Sharpless, V. V. Fokin, *Org. Lett.* **2004**, *6*, 2853–2855.
- [16] P. Appukkuttan, W. Dehaen, V. V. Fokin, E. van der Eycken, *Org. Lett.* **2004**, *6*, 4223–4225.
- [17] C.-Z. Tao, X. Cui, J. Li, A.-X. Liu, L. Liu, Q.-X. Guo, *Tetrahedron Lett.* **2007**, *48*, 3525–3529.
- [18] U. S. Schubert, H. Hofmeier, G. R. Newkome, *Modern Terpyridine Chemistry*, Wiley-VCH, Weinheim, **2006**.
- [19] a) E. Holder, V. Marin, A. Alexeev, U. S. Schubert, *J. Polym. Sci., Part A: Polym. Chem.* **2005**, *43*, 2765–2776; b) A. Winter, U. S. Schubert, *Macromol. Chem. Phys.* **2007**, *208*, 1956–1964.
- [20] S. A. McFarland, F. S. Lee, K. A. W. Y. Cheng, F. L. Cozens, N. P. Schepp, *J. Am. Chem. Soc.* **2005**, *127*, 7065–7070.
- [21] R. T. Brown, N. C. Fletcher, M. Nieuwenhuyzen, T. E. Keyes, *Inorg. Chim. Acta* **2005**, *358*, 1079–1088.
- [22] G. F. Strouse, P. A. Anderson, J. R. Schoonover, T. J. Meyer, F. R. Keene, *Inorg. Chem.* **1992**, *31*, 3004–3006.
- [23] Optical bands gaps have been estimated from the absorption spectra at 10% absorption on the longer-wavelength side.
- [24] Additional investigations (e.g., Raman resonance spectroscopy) will be carried out to further verify this preliminary assumption.
- [25] a) M. A. Bennett, G. Wilkinson, *Chem. Ind.* **1959**, 1516; b) S. Rau, B. Schäfer, A. Grüßing, S. Schebesta, K. Lamm, J. Vieth, H. Görls, D. Walther, M. Rudolph, U. W. Grummt, E. Birkner, *Inorg. Chim. Acta* **2004**, *357*, 4496–4503.

Received: August 1, 2008
 Published online: November 17, 2008